



# CHORUS

This is the accepted manuscript made available via CHORUS. The article has been published as:

## Observation of strong resonant behavior in the inverse photoelectron spectroscopy of Ce oxide

J. G. Tobin, S. W. Yu, B. W. Chung, G. D. Waddill, L. Duda, and J. Nordgren

Phys. Rev. B **83**, 085104 — Published 11 February 2011

DOI: [10.1103/PhysRevB.83.085104](https://doi.org/10.1103/PhysRevB.83.085104)

# Observation of Strong Resonant Behavior in the Inverse Photoelectron Spectroscopy of Ce Oxide

J.G. Tobin<sup>\*,1</sup>, S.W. Yu<sup>1</sup>, B.W. Chung<sup>1</sup>,  
G.D. Waddill<sup>2</sup>, L. Duda<sup>3</sup> and J. Nordgren<sup>3</sup>

1. Lawrence Livermore National Laboratory, Livermore, CA, USA
  2. Missouri University of Science and Technology, Rolla, MO. USA
  3. Uppsala University, Uppsala, Sweden
- \*Contact Author: Tobin1@LLNL.Gov

## Abstract

X-ray Emission Spectroscopy (XES) and Resonant Inverse Photoelectron Spectroscopy (RIPES) have been used to investigate the photon emission associated with the Ce3d<sub>5/2</sub> and Ce3d<sub>3/2</sub> thresholds. Strong resonant behavior has been observed in the RIPES of Ce Oxide near the 5/2 and 3/2 edges.

## I Introduction

Inverse Photoelectron Spectroscopy (IPES) and its high energy variant, Bremsstrahlung Isochromat Spectroscopy (BIS), are powerful techniques that permit a direct interrogation of the low-lying unoccupied electronic structure of a variety of materials. Despite being handicapped by counting rates that are approximately four orders of magnitude less than the corresponding electron spectroscopies (Photoelectron Spectroscopy, PES, and X-ray Photoelectron Spectroscopy, XPS) both IPES [1,2,3,4,5] and BIS [6,7,8] have a long history of important contributions. Over time, an additional variant of this technique has appeared, where the kinetic energy (KE) of the incoming electron and photon energy ( $h\nu$ ) of the emitted electron are roughly the same magnitude as the binding energy of a core level of the material in question. Under these circumstances and

# Observation of Strong Resonant Behavior in the Inverse Photoelectron Spectroscopy of Ce Oxide

in analogy to Resonant Photoelectron Spectroscopy, a cross section resonance can occur, giving rise to Resonant Inverse Photoelectron Spectroscopy or RIPES. [9-13] Here, we report the observation of RIPES in an f electron system, specifically the at the  $3d_{5/2}$  and  $3d_{3/2}$  thresholds of Ce Oxide. (Please see Fig. 1.)

The resonant behavior of the Ce4f structure at the 3d thresholds has been addressed before, including studies of the utilization of the technique as a probe of electron correlation in a variety of Ce compounds. [12] Interestingly, the first RIPES work on rare earths dates back to 1974, albeit under conditions which left the state of the surface and near surface regions undefined. Although they did not use the more modern terminology of "RIPES," it is clear that RIPES was actually first performed in 1974 by Liefeld, Burr and Chamberlain on both La and Ce based materials. [9] In these experiments, the La and Ce metallic samples were attached to the anode of an x-ray tube and the x-ray emission characteristics were measured using a two-crystal monochromator. The pressure in the x-ray tube was quoted as being below  $2 \times 10^{-8}$  Torr. They did indeed observed resonant behavior at the  $M\alpha$  ( $3d_{5/2}$ ) and  $M\beta$  ( $3d_{3/2}$ ) thresholds. In fact, our results here will confirm the measurements made upon the Ce based sample used by Liefeld et al. However, the state of the Ce sample surface and near surface regions are quite undefined in the study in Ref 9. For example, the authors suggest that they are probing Ce metal, since they cannot see any evidence of an  $OK\alpha$  (1s) XES line. However, they do report the observation of a  $FK\alpha$  (1s) line, possibly due to the utilization of cerium fluoride in the sample preparation. Later, they tried to address these issues in a new ultrahigh vacuum system. [13] Based upon our results, it is clear that their

# Observation of Strong Resonant Behavior in the Inverse Photoelectron Spectroscopy of Ce Oxide

original sample surface was oxidized, using the word here in its more general context as in having lost electrons to the oxidizing agent, although whether the structure is an oxide or fluoride remains unclear. In any case, the primacy of Liefeld and coworkers in these measurements should be noted.

Cerium and cerium oxide have been studied with a variety of spectroscopic techniques under UHV conditions. This includes Bremsstrahlung Isochromat Spectroscopy or BIS [6], Photoelectron Spectroscopy [6, 14- 18], X-ray Absorption Spectroscopy [19, 20, 21], Electron Energy Loss Spectroscopy [6,20, 22,23] and Resonant XES [24,25], to name just a few. We will compare our results to those of other spectroscopies, as will be discussed below.

The remainder of this paper will be as follows. In Section II, the experimental details will be described. In Section III, the determination of sample quality with XES and the RIPES results will each be presented and discussed, within the context of the mechanisms of RIPES and XES, as shown in Figure 2. Finally, Section IV will contain a Summary and Conclusions.

## **II Experimental**

The experiments were carried out onsite at Lawrence Livermore National Laboratory, using a spectrometer [26] with capabilities for performing spin resolved Fano spectroscopy [27], high energy Inverse Photoelectron Spectroscopy (IPES) or Bremsstrahlung Isochromat Spectroscopy (BIS), [28] sample cleaning with Argon ion bombardment and sample heating and cooling in an ultra-high vacuum environment.

The polycrystalline Ce sample was oxidized by exposure to air at ambient

## Observation of Strong Resonant Behavior in the Inverse Photoelectron Spectroscopy of Ce Oxide

pressures. After introduction to the ultra-high vacuum system, the oxidized sample was bombarded with Ar ions, to clean the topmost surface regions. The specific details are as follows. The polycrystalline Ce foil (99.9 % of purity, 0.1 mm of thickness, from Alfa Aesar) was cut into a piece with the size of 7x10 mm<sup>2</sup>. One side of the Ce foil was polished with a very fine sandpaper (400 grit), then the sample was oxidized by exposure to air at ambient pressures for about 40 minutes. After introduction to the ultrahigh vacuum, the oxidized sample underwent one set of Ar ion treatment, where it was bombarded with Ar ions (1.7 kV/20 mA,  $p \sim 1 \times 10^{-5}$  torr in the chamber), typically for a period of 30 minutes, multiple times and at nominal room temperature. The sample was not annealed. During these experiments, the XPS capability was unavailable, thus no XPS data were collected on this specific Ce sample. However, based upon previous experience, it is very likely that the sample contained only Ce and O after sputtering with the Ar ions. Therefore, the assertion of cleanliness of the CeOxide sample was indirectly supported by XPS. One set of XES measurements were performed as a test of sample composition and quality, as will be discussed below. Sample stability was addressed via the internal consistency of the sequential BIS/RIPES scans at different kinetic energies.

The XES and IPES/BIS spectra were collected using a Specs electron gun for the excitation and the XES 350 grating monochromator and channel plate system from Scienta as the photon detection. Spectra were collected in “normal mode,” where the electron gun kinetic energy (KE) and the energy position of the center of the channel plate were both fixed and the energy distribution in the

# Observation of Strong Resonant Behavior in the Inverse Photoelectron Spectroscopy of Ce Oxide

photon ( $h\nu$ ) spectrum was derived from the intensities distributed across the channel plate detector in the energy dispersal direction. XES and RIPES data collection occurred with the sample at or near room temperature. In our experiments, the XES spectra play two critical roles: (1) the definition of the location of the resonance in energy space for RIPES and (2) the confirmation of the sample quality. Topic 2 will be discussed below. However, the definition of the absolute energy scale was made with IPES, as will be discussed next.

Energy scale calibration in photoelectron spectroscopy and inverse photoelectron spectroscopy is best performed by direct measurement of the location of the Fermi Edge over a wide series of photon energies. As shown in Figure two, the underlying energy conservation relationship for IPES/BIS is  $h\nu + H^F$  is equal to  $KE + \phi$ , where  $h\nu$  is the photon energy,  $H^F$  is the energy of the empty state (hole) filled, relative to the Fermi Energy ( $E_F$ ),  $KE$  is the Kinetic Energy of the incoming electron and  $\phi$  is some sort of work function. Because the  $KE$  used here is from the output of the electron gun system,  $\phi$  is a spectrometer work function and can contain contact potentials and other offsets. By looking at the Fermi edge,  $H^F$  is set to zero. Unfortunately for CeOxide, the only IPES observed was RIPES, at or near the resonance, as will be discussed below. However, by using the IPES of another material,  $UO_2$ , it was possible to observe Fermi Edges over a wide range and thus calibrate the spectrometer exactly. Initial calibrations of the energy scale, based upon assigning the literature values [29] for the peaks at the Ce  $M\alpha$  ( $3d_{5/2}$ ) and  $M\beta$  ( $3d_{3/2}$ ) thresholds, lead to too large of a spectrometer work function. Using the  $UO_2$  data and a type of linear regression analysis upon the

## Observation of Strong Resonant Behavior in the Inverse Photoelectron Spectroscopy of Ce Oxide

data, a photon monochromator shift,  $\Delta\lambda = 0.35$  angstroms, was determined, which then gave rise to an instrumental work function value of about 2 eV. (See KE = 881 eV in Figure 1.) The same shift of  $\Delta\lambda = 0.35$  was applied to the O1s spectra, with the appropriate scaling with the photon energy squared.

Data collection was performed under ultra-high vacuum conditions. The base pressure of the system was  $3 \times 10^{-10}$  torr, but the pressure changed depending the energy and current of the electron gun. For example, with the XES measurements at KE = 3KeV, the pressure was approximately  $8$  to  $9 \times 10^{-10}$  torr and the excitation current to the sample was typically 0.01 mA, but for RIPES at KE of approximately 900 eV, it was about  $5 \times 10^{-10}$  torr and 0.003 mA. XES data collection required many hours for each spectrum and RIPES spectra took substantially longer.

As will be discussed below, our sample consisted of a thin layer of Ce Oxide lying above Ce metal. Under conditions such as these, thin layers composed of materials that would normally be insulating in the bulk can continue to exhibit a Fermi edge, owing to the thinness of the film and the underlying conductor. [30] It is for this reason that we will refer to the sample as Ce Oxide. Although thermodynamic arguments under oxidizing conditions point to  $\text{CeO}_2$ , it can be argued that "tetravalent"  $\text{CeO}_2$  is unstable and not obtained under these preparation conditions, but only by annealing the sample in an  $\text{O}_2$ -atmosphere. It is very likely that our Ar ion treatment drove the sample into a stable configuration dominated by  $\text{Ce}_2\text{O}_3$ , as reported earlier by Allen. [7] Below, spectroscopic evidence will be presented to support this hypothesis. Next, energy bandpass and

# Observation of Strong Resonant Behavior in the Inverse Photoelectron Spectroscopy of Ce Oxide

broadening effects will be considered.

In general, the observed energy widths in the RIPES and XES experiments follow equation 1 below.

$$\Delta E_{\text{Total}} = \{(\Delta E_{\text{EX}})^2 + (\Delta E_{\text{DET}})^2 + (\Delta E_{\text{LIFE}})^2 + (\Delta E_{\text{CHEM/MULT}})^2\}^{1/2} \quad \text{Eq 1}$$

Here,  $\Delta E_{\text{EX}}$  is the energy broadening from the excitation source, the electron gun.

$\Delta E_{\text{DET}}$  is the broadening from the photon detection, i.e. the monochromator and the multichannel detection of the XES.  $\Delta E_{\text{LIFE}}$  is the intrinsic broadening due to lifetime and other such effects and  $\Delta E_{\text{CHEM/MULT}}$  would be the broadening from the presence of different chemical sites or underlying multiplet structure.

Let us first consider the case of the RIPES experiments, using Figure 1 as a guide. In Figure 1, there is a fairly sharp Fermi edge just below  $h\nu = 885$  eV. The 10%-90% width of a Fermi Edge provides a direct measure of the total energy broadening,  $\Delta E_{\text{Total}}$ . Our measurements indicate that  $\Delta E_{\text{Total}} = 2$  eV, regardless of whether the monochromator entrance slit width was 20 $\mu\text{m}$  or 60 $\mu\text{m}$ . For our monochromator system, it is known that the energy broadening from the photon detection,  $\Delta E_{\text{DET}}$ , should be 0.35 eV for a 20 $\mu\text{m}$  slit width and 1.1 eV for a 60 $\mu\text{m}$  slit width. It is also well known that the intrinsic room temperature width of a Fermi Edge is on the scale of 0.1 eV. Finally, as will be discussed below, this Fermi edge lines up with the higher energy peak in the Ce3d<sub>5/2</sub> XES manifold, indicating that it arises solely from oxide, not metallic Ce. This suggests that here  $\Delta E_{\text{CHEM/MULT}} \cong 0$  eV. Taken together, this indicates the following for the RIPES experiments.

$$\Delta E_{\text{Total}}^{\text{RIPES}} = \Delta E_{\text{EX}}^{\text{RIPES}} = 2 \text{ eV} \quad \text{Eq 2}$$

# Observation of Strong Resonant Behavior in the Inverse Photoelectron Spectroscopy of Ce Oxide

Despite the apparent lack of dependence upon slit size, for some measurements slit sizes were varied, as a test of data set consistency. It is also useful to note that the RIPES spectra exhibit a Fermi edge that is substantially sharper than any features in the XES spectra, as can be seen in Figure 1.

Now, let us consider the XES experiments, again using Figure 1 as a guide. As can be seen easily in the Ce3d<sub>3/2</sub> peak,  $\Delta E_{\text{Total}}^{\text{XES-3/2}} \approx 4 \text{ eV}$ , based upon the full-width-at half-max (FWHM) of the Ce3d<sub>3/2</sub> peak. Here,  $\Delta E_{\text{EX}} = 0 \text{ eV}$ , because, at energies well above the threshold, the excitation energy width used to generate the initial core hole does not effect the decay event energetics. From RIPES energy analysis above, it is known that  $\Delta E_{\text{DET}} \leq 1 \text{ eV}$ . This suggests the following, for the XES-3/2 experiment.

$$\Delta E_{\text{Total}}^{\text{XES-3/2}} = \{(\Delta E_{\text{LIFE}}^{\text{XES-3/2}})^2 + (\Delta E_{\text{CHEM/MULT}}^{\text{XES-3/2}})^2\}^{1/2} \approx 4 \text{ eV} \quad \text{Eq 3}$$

For the XES-5/2 experiment, it is less clear, so a more general equation is required. The impact of these equations will be discussed below.

$$\Delta E_{\text{Total}}^{\text{XES-5/2}} = \{(\Delta E_{\text{DET}}^{\text{XES-5/2}})^2 + (\Delta E_{\text{LIFE}}^{\text{XES-5/2}})^2 + (\Delta E_{\text{CHEM/MULT}}^{\text{XES-5/2}})^2\}^{1/2} \quad \text{Eq 4}$$

## III Spectral Results and Discussion

### IIIa The Resonance Processes

Consider the individual excitation and decay channels for non-resonant XES, IPES, and RIPES, shown below in Equations 5 - 8. The Ce derived valence bands (VB) will include both the 4f and spd states, where the spd states are derived from the 6s, 6p and 5d states. The Ce derived conduction bands (CB), normally empty, will have 4f character as well as spd character. To begin our

# Observation of Strong Resonant Behavior in the Inverse Photoelectron Spectroscopy of Ce Oxide

discussion, let us define the initial state electronic configuration as follows:

$VB^nCB^0$  with  $n \leq 4$ . The different cases discussed below are also schematically illustrated in Figure 2.

## Off Resonance XES: High Energy Excitation and Decay



## On Resonance XES: Excitation and Decay at the Threshold



## Off Resonance IPES and RIPES Direct Channel:



## RIPES Indirect Channel



It is appropriate to begin with XES. When the incoming excitation is at high energies, substantially above the core level binding energy of the 3d levels, then it is expected that the Ce atom will lose a single electron, with a plus 1 change in net charge, with both the excitation electron and 3d core level electron leaving the atom. For example, this occurs when the excitation energy is 3keV or 1.5keV and the core level binding energy is near 900eV. The appropriate relations for this case are shown in Equation 5. However, as the excitation energy is decreased, until it is just above threshold, a different regime is encountered. Here, the excitation electron has only enough energy to lift the 3d core level electron into the previously empty conduction bands, with itself also in the conduction bands. The Ce atom has gained an electron, with the net charge on the atom decreased by

## Observation of Strong Resonant Behavior in the Inverse Photoelectron Spectroscopy of Ce Oxide

one, -1. Very quickly, a decay process can occur, giving rise to the filling of the 3d core hole and the emission of an electron, with a net increase of the occupancy of the Valence Bands by 1, with a retention of the net charge change of  $-1$ . This situation is illustrated in Equation 6. In both limits, the photon emitted in the decay processes, shown in Equations 5b and 6, will have an energy near that of the 3d core level, adjusted for effects such as screening, relaxation and charge.

In IPES, the situation is as follows. Off resonance or regular IPES involves an electron dropping into the conduction band and the emission of a photon. The net charge decreases, by  $-1$ , with the emission of a photon, as summarized in Equation 7. The photon is emitted with an energy that roughly corresponds to the energy of the incoming electron, as shown in Figure 2. ( $\phi$  and  $H^F$  are both small.)

Finally, the case of RIPES is considered here. In RIPES, there are two channels, referred to as direct and indirect. The direct channel, in Equation 7, is the same as the lone channel of off-resonance IPES. The indirect channel, shown in Equation 8, is the same as the near threshold XES of Equation 6. Here, the final state will have a net decrease in charge of  $-1$ , associated with the increase of electron occupancy by 1. The emitted photon energy, 3d core level energy and incoming electron excitation energy must all be approximately equal, as shown in Figure 2.

In the present study, the process of Resonant Inverse Photoemission is being invoked to explain the experimental observations. However, the corresponding resonant process in the photoemission of Ce has been studied for

## Observation of Strong Resonant Behavior in the Inverse Photoelectron Spectroscopy of Ce Oxide

many years. In fact, resonant photoelectron spectroscopy (RES-PES) at the Ce 4d and 3d thresholds was performed decades ago by J.W. Allen [7], C. Laubschat et al. [31], and the group of S. Suga. [32] Here, the interference of the direct photoemission channel and an indirect channel, using a d-4f dipole excitation followed by a decay that ends up in the same final state as the direct process, can give rise to an interference that leads on-resonance to a strong enhancement of the Ce 4f emission. In this study, the inverse process is considered, specifically the interference of the direct IPES direct channel and an IPES indirect channel, driven by an electron induced 3d excitation and followed by a dipole transition. As in the case of the PES process resonance, the IPES process resonance will hinge upon the f-d dipolar transition. The indirect IPES channel will be dominated by a 4f to 3d transition, following electric dipole selection rules and generating the emission of a photon. Similarly, it is reasonable to expect that the excitation will be dominated by 3d to 4f transitions, driven by the large density of empty 4f states and their spatial localization close to the 3d orbitals, despite the lessened selectivity of the coulombic matrix elements associated with excitation by kilovolt range electrons. Thus, the key to resonance is the d-f dipolar transitions.

Now, let us return to a consideration of the nature of the Ce oxide valence and conduction bands. In metallic Ce, something like  $4f^1(sp d)^3CB^0$  would be expected, reflecting the notion that Ce metal is “trivalent.” If the CeOxide were  $CeO_2$  and were completely ionized, then  $4f^0(sp d)^0CB^0$  would be expected. This is the so-called “formal charge,” which assumes complete success by the oxidizing agent in the ionization process. If the CeOxide were  $Ce_2O_3$  and were completely

# Observation of Strong Resonant Behavior in the Inverse Photoelectron Spectroscopy of Ce Oxide

ionized, again a “formal charge,” then  $4f^{1-x}(spd)^x CB^0$  would be expected, with  $x$  near or at zero. However, the CeOxide is probably only partially oxidized and partially ionized, with a possible component of covalency and partial occupation. Thus, whether the CeOxide is either  $CeO_2$  or  $Ce_2O_3$ , it is not unreasonable to expect the Ce valence and conduction bands to be something like  $4f^{1-a}(spd)^{3-b} CB^0$ , with  $0 \leq a \leq 1$  and  $0 \leq b \leq 3$  and  $a + b \leq 4$  for  $CeO_2$  and  $a + b \leq 3$  for  $Ce_2O_3$ . It is also reasonable to expect the spd states to ionize more easily than the 4f states. Hence, one would expect the following:  $3-b < 1-a$ . In any case, there will be no shortage of unoccupied 4f states for the excitation process: there will be a minimum of 13 and a maximum of 14. However, while it is possible that the 4f electron generated by the excitation will also participate in the decay, any additional original occupation of the Ce 4f states would probably strongly enhance the decay process. Thus, the observation of a resonant effect in the RIPES of CeOxide strongly favors the assignment of the CeOxide as  $Ce_2O_3$ , and not  $CeO_2$ . Lastly, the interpretation of the resonance as arising from  $Ce_2O_3$  is consistent with the earlier observations by J.W. Allen of a strong 4d Res-Pes effect in  $Ce_2O_3$ . [7]

## IIIb Confirmation of Sample Quality

XES of the Ce  $3d_{5/2}$ , Ce  $3d_{3/2}$  and O1s levels were used to characterize the Ce Oxide sample. As shown in Figure 1, there are two components to the  $M\alpha$  ( $3d_{5/2}$ ) peak but only one for the  $M\beta$  ( $3d_{3/2}$ ) peak. This is not surprising: the larger lifetime broadening associated with the  $M\beta$  ( $3d_{3/2}$ ) threshold can smear out fine structure. Some of the processes involved in the production of these spectral features can be seen in Figure 2. Because  $3d_{3/2}$  states are at a higher binding

## Observation of Strong Resonant Behavior in the Inverse Photoelectron Spectroscopy of Ce Oxide

energy relative to the Fermi Level ( $B^F$ ) than the  $3d_{5/2}$  states, a fast, non-radiative decay through the  $3d_{5/2}$  states is possible, contributing to the broadening.

Furthermore, decay channels such as this can also explain the divergence of the peak intensities from the “statistical” limit, where intensity should scale with the number of states. In this limit, the ratio of the intensities,  $3d_{5/2}$  versus  $3d_{3/2}$  should be 3:2. The observed intensity ratio is quite a bit larger, as can be seen in Figure 1. Next, we will use the KE dependence of the excitation to probe the origin of the splitting in the  $3d_{5/2}$  peak and relate that to the sample structure.

As shown in Figure 3, it is possible to induce changes in the relative intensities of the two components in the Ce  $3d_{5/2}$  spectral feature. These two components will be assigned to the underlying Ce metal and the near surface Ce Oxide thin film. There are two data sets shown in Figure 3, corresponding to two different slit sizes for the monochromator. Temporally, these four spectra were taken one after the other, contiguously. In both cases, lowering the KE from 3KeV to 1.5 KeV enhances the second component of the Ce  $3d_{5/2}$  spectral feature. Under these conditions, the escape depths of the photons should not be a factor, but the penetration depths of the electrons should. By lowering the KE, the surface sensitivity is increased. This argues for the material associated with the sub-peak at the lower photon energy to be underneath the material associated with the sub-peak at the higher photon energy. It is reasonable to assume that the underlying material is metallic Ce and that the layer above it is oxidized Ce. This assignment is confirmed by a consideration of the literature and previous experiments. It was shown earlier by Baer and coworkers [6] that  $CeO_2$  exhibited additional spectral

## Observation of Strong Resonant Behavior in the Inverse Photoelectron Spectroscopy of Ce Oxide

structure in XPS and EELS at higher binding energies, relative to Ce metal. This result has been confirmed by others, using XPS [18] and EELS [22]. Similar intensity shifts to higher energies has been observed in XAS as well. [19] In fact, as part of a previous collaboration [20], we have observed this shift before, utilizing XAS on Beamline 8 at the Advanced Light Source. [21] Using oxidized bulk Ce samples, it was possible to see strong, shifted spectral structure which could be removed by scraping, giving rise to a final XAS result which approximated the evaporated samples utilized in our other study. [20] Thus, there is very strong evidence to support the assignment of the lower photon energy sub-peak in the Ce  $3d_{5/2}$  manifold to the underlying bulk metallic Ce and the higher photon energy sub-peak to a near surface layer of CeOxide. Additionally, it should be noted that there appears to be a very weak enhancement of a low hv shoulder on the Ce $3d_{3/2}$  peak, as the KE is increased from 1.5 KeV to 3 KeV. This lower hv shoulder would correspond to the Ce metal Ce $3d_{3/2}$  contribution. However, the enhancement of the shoulder in the Ce $3d_{3/2}$  peak is very weak and should be regarded with caution. The larger lifetime broadening expected for the lower j component of the spin orbit split doublet appears to smear out any underlying fine structure.

Now, let us consider the changes in peak shape as a function of slit width. In both cases, for KE = 1.5 KeV and KE = 3.0 KeV, in going from a slit width of 20  $\mu\text{m}$  to 60  $\mu\text{m}$ , the peak height of the Ce metal  $3d_{5/2}$  peak increases noticeably, with a corresponding change in peak shape. The rest of the spectra remain essentially the same: the Ce $3d_{3/2}$  peak and the Ce oxide  $3d_{5/2}$  subpeak. We believe these observations are a function of the interplay of lifetime broadening and the

## Observation of Strong Resonant Behavior in the Inverse Photoelectron Spectroscopy of Ce Oxide

monochromator energy resolution bandpass. Consider equation 3, above. For the Ce3d<sub>3/2</sub> peak, we concluded that the peak width was driven by lifetime broadening and underlying structure due to chemical shifts and multiplet structure. However, we also note above that the high hv shoulder in the Ce3d<sub>3/2</sub> peak is very weak. Furthermore, the triangular peak shape is consistent with the Lorentzian function associated with lifetime broadening. Thus, the energy-width in the Ce3d<sub>3/2</sub> peak is dominated by lifetime effects. This result is shown in equation 9 below.

$$\Delta E_{\text{Total}}^{\text{XES-3/2}} = (\Delta E_{\text{LIFE}}^{\text{XES-3/2}}) \approx 4 \text{ eV} \quad \text{Eq 9}$$

Equation 9 implies that the Ce3d<sub>3/2</sub> peak should be independent of the slit width. The spectra in Figure 3 are consistent with this assertion. Thus, it is justified to use the height of the Ce3d<sub>3/2</sub> peak as a type of normalization.

Next, the sub-peaks in the Ce3d<sub>5/2</sub> peak will be considered. Because the two sub-peaks overlap, the analysis will need to be couched in terms of the half-widths-at half-maximum (HWHM), using the outside halves of each sub-peak for the analysis. Also, because the sub-peaks are being separated upon the basis of their chemical origin, it will be assumed that the  $\Delta E_{\text{CHEM/MULT}}$  can be neglected. For the case of the CeOxide Ce3d<sub>5/2</sub> peak, it can be seen that the peak is essentially constant, regardless of slit width and KE, relative to the Ce3d<sub>3/2</sub> peak. The peak height remains fairly uniform and the triangular/Lorentzian peak shape is robustly retained, with a HWHM also on the same scale as that of the Ce3d<sub>3/2</sub> peak. This strongly suggests that the CeOxide Ce3d<sub>5/2</sub> peak is also dominated by lifetime effects, with no dependence upon any internal structure or the monochromator resolution.

## Observation of Strong Resonant Behavior in the Inverse Photoelectron Spectroscopy of Ce Oxide

$$\Delta E_{\text{Total-CeOxide}}^{\text{XES-5/2}} = \Delta E_{\text{LIFE-CeOxide}}^{\text{XES-5/2}} \quad \text{Eq 10}$$

Interestingly, both the XAS work by Kaindl et al [19] and our unpublished work [20,21] suggest that the CeOxide Ce3d<sub>5/2</sub> peak has a line-shape and line-width quite similar to that of the CeOxide Ce3d<sub>3/2</sub> peak, while the Ce metal Ce3d<sub>5/2</sub> peak has more internal fine structure and a more sharply rising line-shape than the corresponding Ce metal Ce3d<sub>3/2</sub> peak. This would be consistent with a lifetime broadening limit in the CeOxide Ce3d<sub>5/2</sub> peak but a possible dependence upon both lifetime broadening and instrumental broadening in the Ce metal Ce3d<sub>5/2</sub> peak. Thus, for the Ce metal Ce3d<sub>5/2</sub> peak, the following is appropriate.

$$\Delta E_{\text{Total-Ce metal}}^{\text{XES-5/2}} = \{ (\Delta E_{\text{DET}}^{\text{XES-5/2}})^2 + (\Delta E_{\text{LIFE-Ce metal}}^{\text{XES-5/2}})^2 \}^{1/2} \quad \text{Eq 11}$$

From Equation 11, a lifetime broadening of about 1 to 2 eV can be obtained. This has been done using (1) a simple line-shape model that assumes an inverse proportionality between peak height and peak width, for constant peak area; (2) the experimentally observed peak height increase of approximately 1/4 between the 20μm and 60μm spectra of Figure 3; and (3) the values of ΔE<sub>DET</sub>(20μm) ≈ 0.35 eV and ΔE<sub>DET</sub>(60μm) ≈ 1.1 eV. This result is shown in Equation 12.

$$1 \text{ eV} \leq \Delta E_{\text{LIFE-Ce metal}}^{\text{XES-5/2}} \leq 2 \text{ eV} \quad \text{Eq 12}$$

The total line-widths from this model would be on the scale of 2 eV to 3eV, in accord with the spectra in Figure 3. This result in Equation 12 is consistent with the earlier XAS results and explains the increase in the peak height of the Ce metal Ce3d<sub>5/2</sub> peak relative to the other constant spectral features.

The above interpretation is further supported by the O1s XES data plotted in

## Observation of Strong Resonant Behavior in the Inverse Photoelectron Spectroscopy of Ce Oxide

Figure 4. First, there can be no doubt that this sample is an oxide of some sort: a strong O1s spectral feature is clearly evident. Second, the result is independent of electron excitation energy, for both data sets with different slit sizes, indicating that all of the oxygen is at or near the surface, not in the bulk. Third, most of the intensity is in the main feature at a photon-energy of 524 eV. This main feature is assigned to the near surface thin film of CeOxide. The second, smaller feature near 526 eV is associated with true surface oxygen, possibly physically or chemically attached to the top of the CeOxide layer. It is reasonable to expect that the physically or chemically attached oxygen may be in a higher oxidation state, i.e. without the oxidized electrons from Ce, and would thus be at a higher photon energy. [Since oxygen is the oxidizing agent, it is the Ce that gets oxidized and the oxygen that gets reduced. A reduced atom may have less of a tight hold upon its electrons, thus giving rise to a lower binding energy. Hence, the oxygen in CeOxide is expected to have a lower O1s binding energy than the physically or chemically absorbed oxygen species.]

Thus, supported by the XES results, our picture is the following. The bulk Ce is coated with a thin film of Ce Oxide, but thin enough that we see the retention of a Fermi Edge in the RIPES spectra.

Finally, before going on to a discussion of the RIPES results, there is one last feature to discuss in the XES spectra in Figures 1 and 3. In the XES spectra there are also the weak features near 865 eV and 905 eV. Because our data collection is performed in normal mode, it is possible that weak features such as these are artifacts of the monochromator and/or channel plate signature. Because

# Observation of Strong Resonant Behavior in the Inverse Photoelectron Spectroscopy of Ce Oxide

of their weakness, a further analysis was not pursued. Next, the RIPES spectra will be described and discussed.

## IIIc RIPES of the Ce 3d states

A strong resonance in the RIPES of Ce Oxide has been observed. Here, we will present the experimental XES and RIPES data and discuss them within the framework of previous results.

As shown in Figure 1, the RIPES and XES are coincident in energy space. This coincidence is independent of any energy scale calibration, because the same monochromator settings were used in each data collection. Only the energy of the incoming excitation electrons was changed. The difference in the spectra is due to the change in the energy of the incoming beam. For the XES, the excitation beam is at an energy of 3KeV, well above the Ce  $M\alpha$  ( $3d_{5/2}$ ) and  $M\beta$  ( $3d_{3/2}$ ) thresholds. As illustrated in Figure 2, the electron beam serves only to scatter off of the core level electrons and generate a core hole, beginning the process that ultimately gives rise to the photon emission at the characteristic energies associate with XES. Using the XES as a guide, a photon energy window was thus chosen for the RIPES experiments. As can be seen in Figure 1, the RIPES spectrum at KE = 881 eV is much sharper than the XES spectrum. Consistent with the picture shown in Figure 2, there is no intensity at the higher photon energies, above  $E_F$ . This is because the transitions in this regime would correspond to the incoming electron dropping into an occupied state, which is forbidden. The intensity jump occurs at  $E_F$  and continues into the regime where  $H^F$  is greater than zero, where the incoming electron is dropping into the unoccupied conduction band. The defining

## Observation of Strong Resonant Behavior in the Inverse Photoelectron Spectroscopy of Ce Oxide

characteristic of IPES is that  $KE \approx hv$ . For RIPES to occur, a second, indirect channel must open up, providing an additional path into the final state associated with IPES. There are further, quantum-mechanically-driven aspects to a resonance, but that discussion can be found elsewhere. [7, 31,32,33]

Energetically, the defining characteristic of being on resonance is that  $KE \approx B^F$ , the core level binding energy relative to the Fermi Level,  $E_F$ . Thus for RIPES,  $hv \approx KE \approx B^F$ , as presented schematically in Figure 2. As the photon energy is diminished further, the RIPES intensity drops, with the final state moving out of the higher density conduction bands and into the less dense, more-free-electron-like states.

Spectral summaries of the RIPES and XES are shown in Figures 5 and 6, for the Ce  $3d_{5/2}$  and Ce  $3d_{3/2}$  thresholds. In both cases, it is clear that the resonance occurs only within the confines of the energy regime defined by the XES spectrum. Each time, the resonance begins to turn on as the excitation kinetic energy (KE) approaches the photon energy associated with the XES peak. The maxima are obtained when the KE reaches approximate equivalence with the photon energy associated with the corresponding XES peak. As mentioned before, in the Ce $3d_{5/2}$  regime, the resonance is associated with only the CeOxide XES peak, not the Ce metal XES peak at lower photon energies. In the case of the Ce $3d_{3/2}$  regime, the separation of the metal and oxide contributions is lost, presumably due to the increased lifetime broadening of the 3/2 feature.

It is of interest to look carefully at the photon energy dependence of the IPES. For the Ce  $3d_{5/2}$ , there appear to be weak intensities at  $KE = 877, 878, 886$

## Observation of Strong Resonant Behavior in the Inverse Photoelectron Spectroscopy of Ce Oxide

and 887 eV, that suggest off-resonance spectral structure, shifting with KE. This would be the spectral dispersion of the IPES Fermi Edge, driven by the linear relationship between  $h\nu$  and KE, as shown in Figure 2. In the intervening KE's, the resonance is dominant and the intensity reflects not so much Fermi Edge dispersion with the changing KE but instead the onset and subsequent diminishment of a peak with a fixed high energy cutoff, as it moves through resonance with a maximum at KE = 881 eV. In the regime of KE = 879 to 885 eV in Figure 5, it is clear that the leading edge of the peak does not move. This leading edge is the Fermi edge at the resonant energy, KE = 881 eV, which is directly below the peak in the CeOxide XES feature, as shown in Figures 1 and 5. At lower KE's, 879 – 881 eV, the width of the main feature diminishes with increasing KE. This suggests that a regular IPES peak is walking up to the resonance and then becoming energy coincident and integrally part of the resonance at 881 eV. At energies above the resonance, 883 – 885 eV, the width of the spectra feature again diminishes, suggesting that the resonance is persisting as the tail of the IPES peak but with a cut-off corresponding to the KE = 881 eV Fermi edge. Finally, at KE = 886 and 887 eV, there may actually be a shift in the Fermi edge position with increasing KE, although with much weaker intensity. A similar process occurs for the Ce  $3d_{3/2}$  resonance, with a maximum of the higher photon energy peak occurring at KE near 900 eV. Again, in the regime of KE = 897 to 903 eV, as the main peak walks up in photon energy and the resonance occurs, the peak width narrows as the peak position moves toward the cutoff at the Fermi edge associated with the resonance maximum at KE = 900 eV. The Ce

## Observation of Strong Resonant Behavior in the Inverse Photoelectron Spectroscopy of Ce Oxide

$3d_{3/2}$  RIPES is complicated by the presence of a Ce  $3d_{5/2}$  peak. This is the RIPES manifestation of the non-radiative decay process shown in Figure 2. Thus, some of the Ce  $3d_{3/2}$  RIPES intensity is lost to this XES-like feature. It is interesting that at the KE's below the threshold for resonance in the Ce $3d_{3/2}$  regime, e.g. KE = 895 eV and 896 eV, the XES-like feature associated with the Ce $3d_{5/2}$  energy dominates the spectra. As the Ce $3d_{3/2}$  resonance turns on, the feature at the Ce  $3d_{3/2}$  energy becomes dominant, but the Ce $3d_{5/2}$  peak persists. Above the resonance, at KE = 905 eV, the envelope of the spectrum becomes similar to that observed at much higher excitation energies, i.e. KE = 1.5 KeV and 3 KeV. (Figure 3) Again, there is some evidence of weak dispersion of the Fermi Edge, at kinetic energies below (KE = 895 and 896 eV) and above (KE = 904 and 905 eV) the resonant regime.

As described above, the resonance is associated with the CeOxide and not the metallic Ce. This interpretation is confirmed by a consideration of the spectra shown in Figure 7. Here, the results of measurements of metallic Ce, carried out in a similar spectrometer, are presented. [34,35] The resonance appears to be far weaker in the metallic Ce than in the CeOxide. The picture of resonance enhancement with the transition from delocalized to localized behavior is not new and this interpretation is consistent with a picture put forward earlier by Dowben. [36] In Dowben's picture, delocalization serves to provide alternate, inter-atomic decay-channels, that tend to subtract from the resonant enhancement. Localization maximizes the resonance by restricting access to these additional

# Observation of Strong Resonant Behavior in the Inverse Photoelectron Spectroscopy of Ce Oxide

channels, instead optimizing the decay via the indirect, intra-atomic channel (Figure 2) that is energy-coincident with the IPES direct channel.

Finally, it is useful to compare our results to those of Liefeld, Burr and Chamberlain. [9] Our RIPES spectroscopic results are in essentially complete agreement with theirs. The photon energy dependences at both the Ce  $M\alpha$  ( $3d_{5/2}$ ) and  $M\beta$  ( $3d_{3/2}$ ) thresholds are same. Thus it seems very unlikely that the source of their RIPES was Ce metal, but rather is some sort of oxidized Ce, although the exact nature of the oxidation, either cerium oxide or cerium fluoride, remains unknown.

## IV Summary and Conclusions

Strong resonant behavior in the Inverse Photoelectron Spectroscopy of a thin layer of CeOxide, near the Ce 3d edges, has been observed. It confirms the picture of resonance enhancement with localization and explains the observations of Liefeld, Burr and Chamberlain from 35 years ago.

## Acknowledgements

Lawrence Livermore National Laboratory is operated by Lawrence Livermore National Security, LLC, for the U.S. Department of Energy, National Nuclear Security Administration under Contract DE-AC52-07NA27344. This work was supported by the DOE Office of Science, Office of Basic Energy Science, Division of Materials Science and Engineering. We would like to thank Emiliana Damian-Risberg for her work on the experiments in Sweden, Jonathan Denlinger for his help with the Beamline 8 experiments at the ALS and Thorsten Schmitt and Jinghua Guo for their mentoring of E. D.-R.

# Observation of Strong Resonant Behavior in the Inverse Photoelectron Spectroscopy of Ce Oxide

## References

1. G. Denninger, V. Dose, and H. P. Bonzel, Phys. Rev. Lett. **48**, 279 (1982); V. Dose, Appl. Phys. **14**, 117 (1977).
2. P. D. Johnson and N. V. Smith, Phys. Rev. Lett. **49**, 290 (1982).
3. F. J. Himpsel and Th. Fauster, Phys. Rev. Lett. **49**, 1583 (1982).
4. B.J. Knapp and J.G. Tobin, Phys. Rev. B **37**, 8656 (1988).
5. J.G. Tobin, "Photoemission and Inverse Photoemission," in "Determination of Optical Properties," Vol. VIII in Physical Methods of Chemistry, 2nd edition, Ed. B.W. Rossiter and R.C. Bretzold, John Wiley and Sons, New York, 1993 and references therein.
6. E. Wuilloud, B. Delley, W.D. Schneider, and Y. Baer, Phys. Rev. Lett. **53**, 202 (1984); E. Wuilloud, H.R. Moser, W.D. Schneider, and Y. Baer, Phys. Rev. B **28**, 7354 (1983).
7. J.W. Allen, J. Magn. Mat. **47/48**, 168 (1985); J. Less-Com. Met. **93**, 183 (1983).
8. P. Kuiper, J. van Elp, G.A. Sawatzky, A. Fujimori, S. Hosoya, and D.M. de Leeuw, Phys. Rev. B **44**, 4570 (1991).
9. R. J. Liefeld, A.F. Burr and M.B. Chamberlian, Phys. Rev. A **9**, 316 (1974); M.B. Chamberlain, A.F. Burr, and R.J. Liefeld, Phys. Rev. A **9**, 663(1974).
10. F. Reihle, Phys. Status Solidi **98**, 245 (1980).
11. Y.Hu, T.J. Wagener, Y. Gao, J.H. Weaver, Phys. Rev B **38**, 12709 (1988).
12. P. Weibel, M. Grioni, D. Malterre, B. Dardel, and Y. Baer, Phys. Rev. Lett. **72**, 1252 (1994); M. Grioni, P. Weibel, D. Malterre, Y. Baer, and L. Du`o, Phys. Rev. B **55**, 2056 (1997).

## Observation of Strong Resonant Behavior in the Inverse Photoelectron Spectroscopy of Ce Oxide

13. B.E. Mason, R.J. Liefeld, *J. Vac. Sci. Tech. A* **8**, 4057 (1990).
14. D. Wieliczka, J. H. Weaver, D. W. Lynch, and C. G. Olson, *Phys. Rev. B* **26**, 7056 (1982)
15. E. Vescovo and C. Carbone, *Phys. Rev. B* **53**, 4142 (1996).
16. E. Weschke, C. Laubschat, T. Simmons, M. Domke, O. Strebels, and G. Kaindl, *Phys. Rev. B.* **44**, 8304 (1991).
17. P. Pasala, S. Logothetidis, L. Sygellou and S, Kennou, *Phys. Rev. B* **68**, 035104 (2003).
18. N.A. Braaten, J.K. Grepstad, and S. Raaen, *Phys. Rev. B* **40**, 7969 (1989).
19. a. G. Kaindl, G. Kalkowski, W.D. Brewer, E.V. Sampathkumaran, F. Holtzberg, A. Schach v. Wittenau, *J. Mag. Mag. Matl.* 47/48, 181 (1985); b. C. Bonnelle, R.C. Karnatak, and J. Sugar, *Phys. Rev. A* **9**, 1920 (1974).
20. K.T. Moore, B.W. Chung, S.A. Morton, S. Lazar, F.D. Tichelaar, H.W. Zandbergen, P. Söderlind, G. van der Laan, A.J. Schwartz, and J.G. Tobin, *Phys. Rev. B* **69**, 193104 (2004).
21. J. Denlinger, private communication, December 2009.
22. J. Bloch, N. Shamir, M.H. Mintz and U. Atzmony, *Phys. Rev. B.* **30**, 2462 (1984).
23. Lijun Wu, H.J. Wiesmann, A.R. Moodenbaugh, R.F. Klie, Yimei Zhu, D.O. Welch and M. Suenaga, *Phys. Rev. B* **69**, 125415 (2004).
24. C. Dallera, M. Grioni, A. Palenzona, M. Taguchi, E. Annese, G. Ghiringhelli, A. Tagliaferri, N. B. Brookes, Th. Neisius, and L. Braicovich, *Phys. Ev. B* **70**, 085112 (2004).

## Observation of Strong Resonant Behavior in the Inverse Photoelectron Spectroscopy of Ce Oxide

25. M. Watanabe, Y. Harada, M. Nakazawa, Y. Oshiwata, R. Eguchi, T. Takeuchi, A. Kotani and S. Shin, Surf. Rev. Lett. **9**, 983 (2002).
26. J.G. Tobin, S.W. Yu, T. Komesu, B.W. Chung, S.A. Morton, and G.D. Waddill, Matl. Res. Soc. Symp. Proc. **986**, 63 (2007).
27. S.W. Yu and J. G. Tobin, Phys. Rev. B **77**, 193409 (2008); S.W. Yu and J.G. Tobin, Surface Science Letters **601**, L127 (2007).
28. J.G. Tobin, S.-W. Yu, B.W. Chung, G.D. Waddill and AL Kutepov, IOP Conf. Series: Matl Sci and Eng **9**, 012054 (2010); doi:10.1088/1757-899X/9/1/012054
29. X-ray Data Handbook, A. Thompson et al, LBNL, Berkeley, CA,USA, Jan 2001.
30. B.W. Veal and D.J. Lam, Phys. Rev. B **10**, 4902 (1974) and Phys. Letters **49A**, 466 (1974).
31. C. Laubschat, E. Weschke, G. Kalkowski, and G. Kaindl, Physica Scripta **41**, 124 (1990); C. Laubschat, E. Weschke, C. Holtz, M. Domke, O. Strebel and G. Kaindl, Phys. Rev. Lett. **65**, 1639 (1990).
32. R.-J. Jung et al., Phys. Rev. Lett. **91**, 157601 (2003), S.-J. Oh et al, Solid State Commun. **82**, 581 (1992).
33. S.R. Mishra, T.R. Cummins, G. D. Waddill, W.J. Gammon, G. van der Laan, K.W. Goodman, and J.G. Tobin, Phys. Rev. Lett. **81**, 1306 (1998).
34. Emiliana Damian, "X-ray Emission Spectroscopy Applied in materials Science," Uppsala University, Uppsala, Sweden.
35. L. Duda, <http://homepage.mac.com/lcduda/RIPES1.html>
36. P.A. Dowben, Surface Science Reports **40**, 151 (2000).

# Observation of Strong Resonant Behavior in the Inverse Photoelectron Spectroscopy of Ce Oxide

## Figure captions

Figure 1

The XES and RIPES of Ce Oxide is shown here.

Figure 2

Schematic models for the processes of XES and RIPES are illustrated here.

Figure 3

The XES of the Ce 3d states is plotted here, including their dependences upon kinetic energy (KE) and the monochromator entrance slit width. The spectra were normalized to the Ce3d<sub>3/2</sub> peak heights. See text for details.

Figure 4

The XES of the O1s is shown here.

Figure 5

A plot of both the XES and RIPES near the Ce 3d<sub>5/2</sub> threshold is shown here, including the photon energy dependence of the Ce 3d<sub>5/2</sub> RIPES resonance.

Figure 6

A plot of both the XES and RIPES near the Ce 3d<sub>3/2</sub> threshold is shown here, including the photon energy dependence of the Ce 3d<sub>3/2</sub> RIPES resonance.

Figure 7

The RIPES and XES of Ce metal are shown here. [34,35]

# CeOxide XES & RIPES

XES  
KE = 3 KeV

Ce3d<sub>5/2</sub>  
880 eV

Ce3d<sub>3/2</sub>  
898 eV

RIPES  
KE = 881 eV  
 $\Delta E = 2$  eV

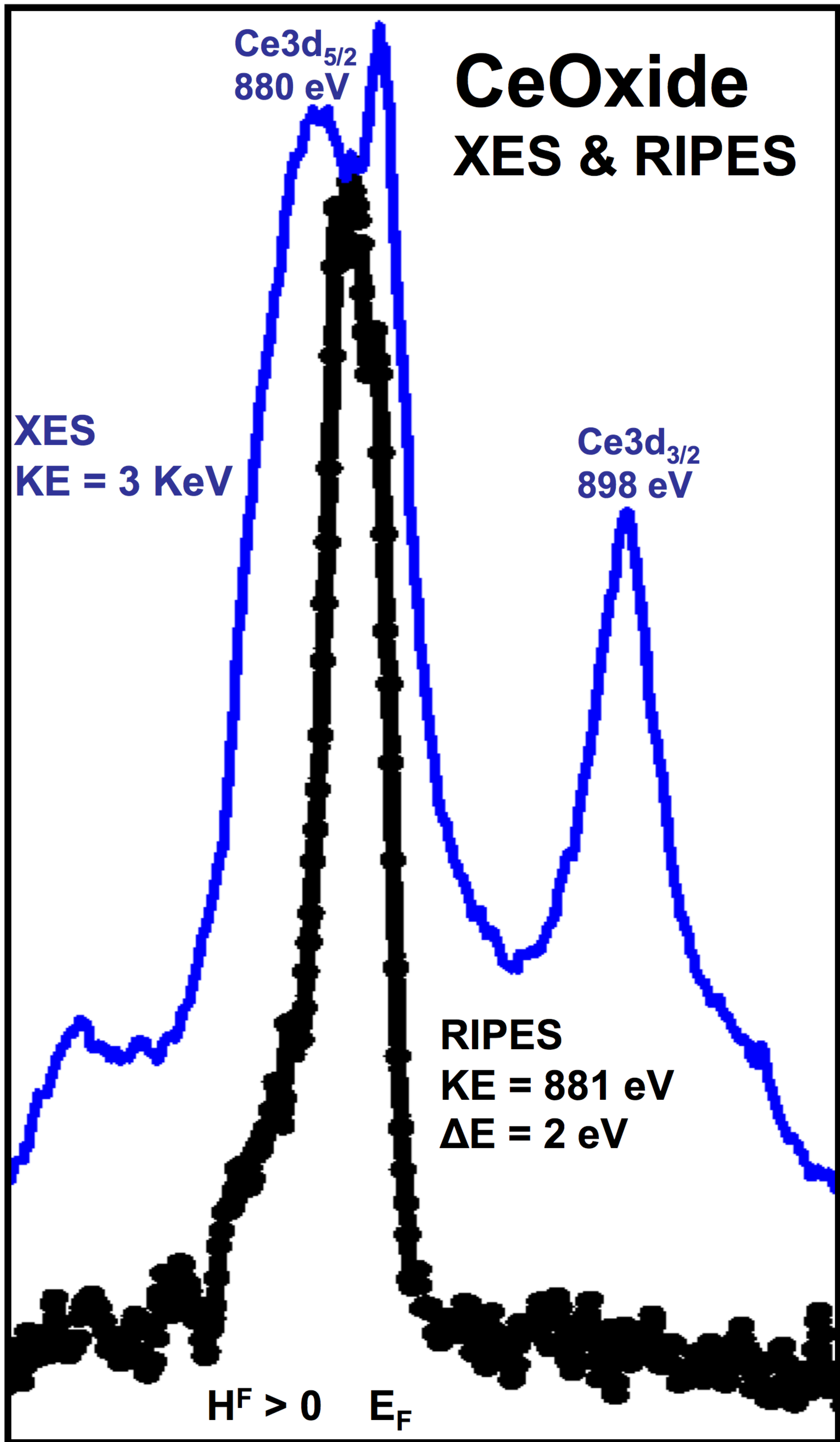
H<sup>F</sup> > 0    E<sub>F</sub>

860

885

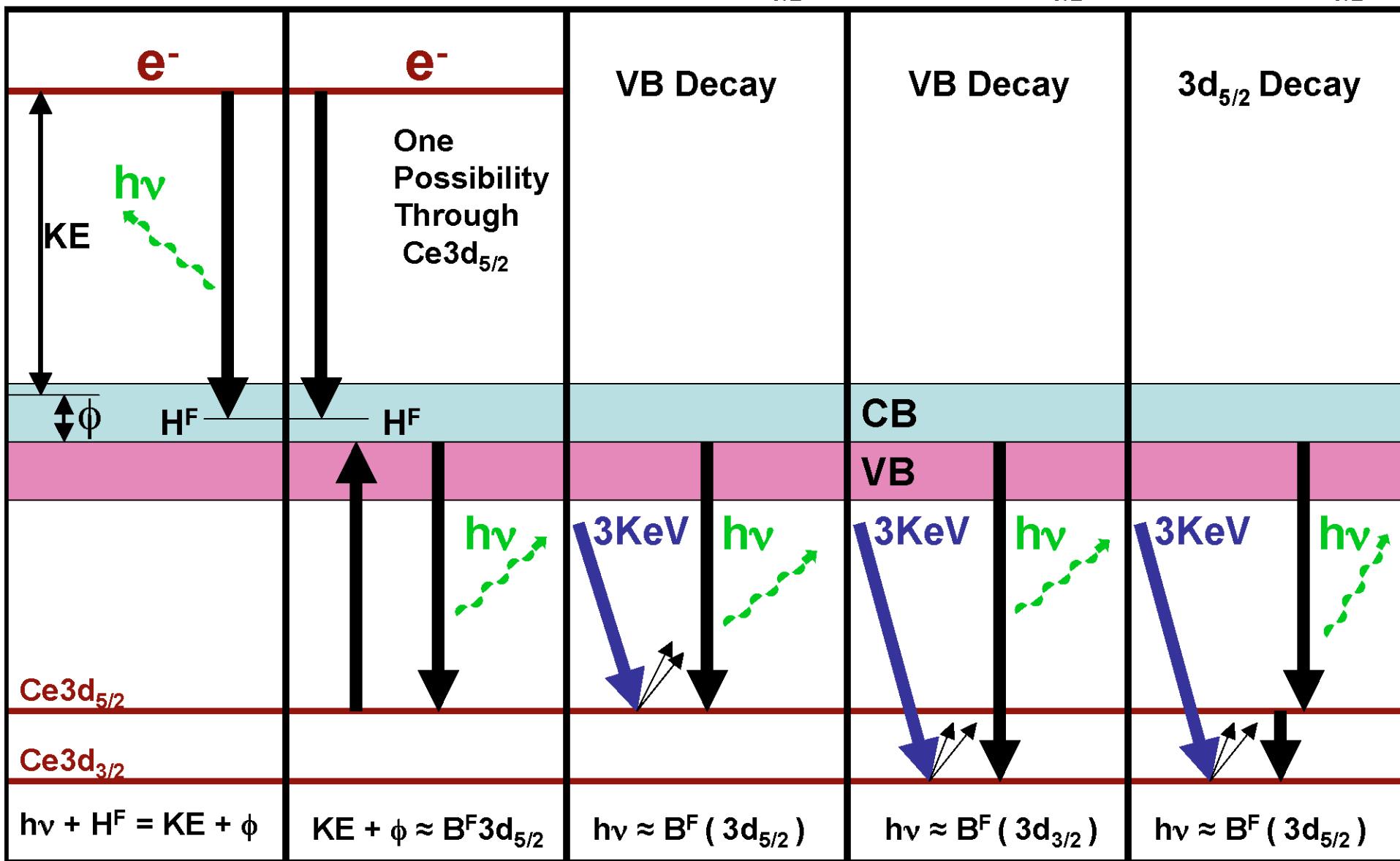
910

Photon Energy (eV)



RIPES-Direct

RIPES-Indirect

XES Ce3d<sub>5/2</sub>XES Ce3d<sub>3/2</sub>XES Ce3d<sub>3/2</sub>

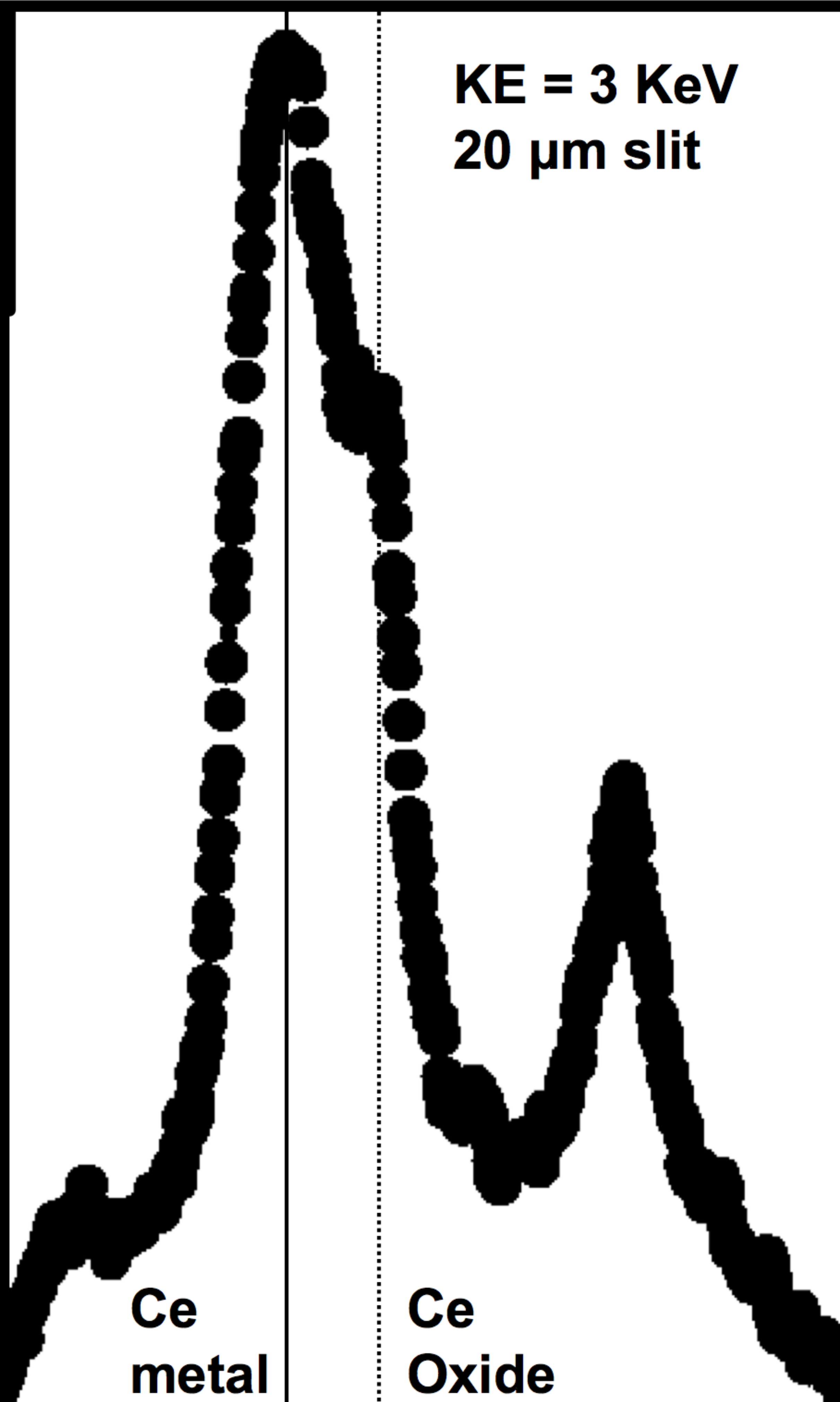
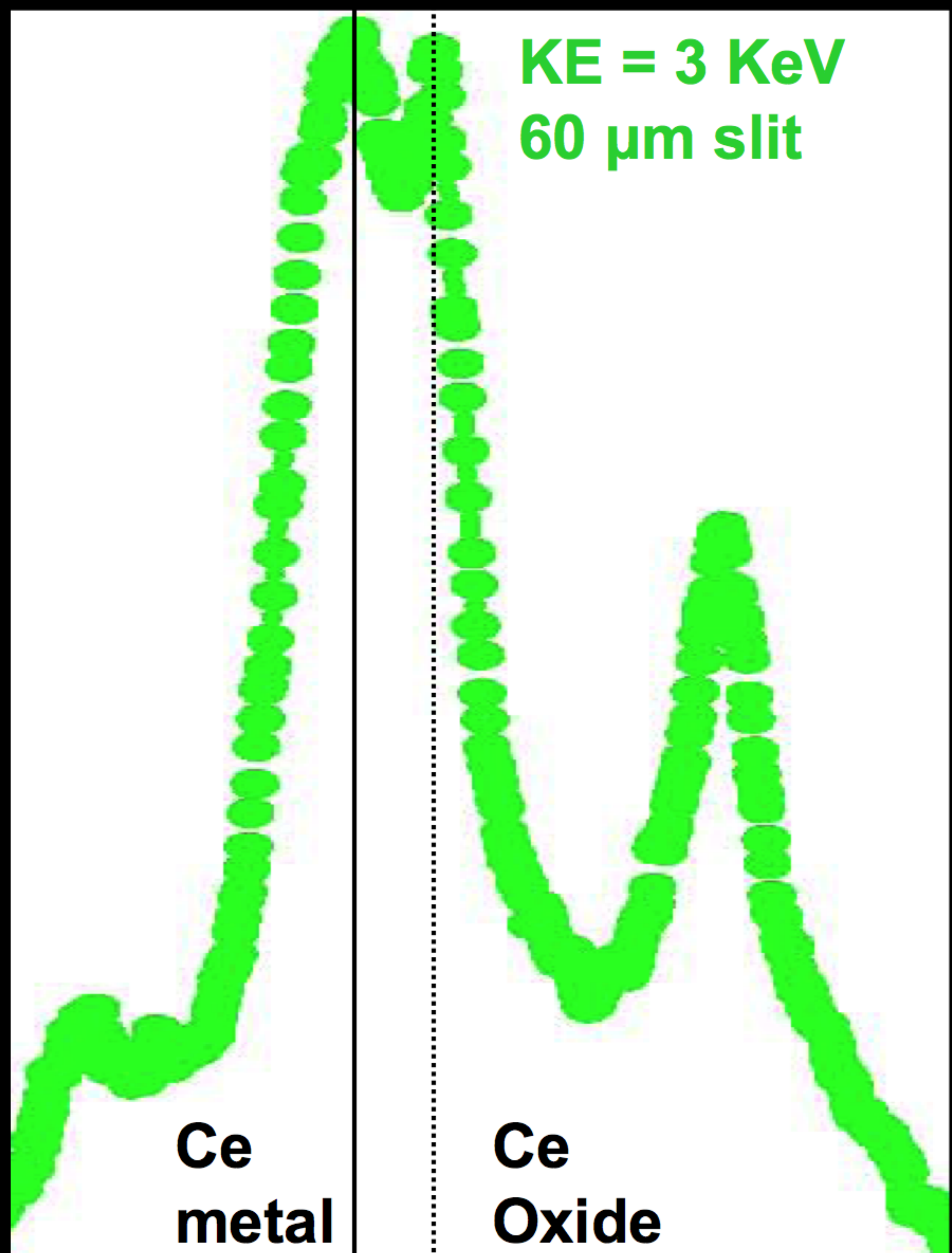
# Ce 3d (M) XES

## KE and slit width

Intensity (Arb. Units)

KE = 3 KeV  
20  $\mu\text{m}$  slit

KE = 3 KeV  
60  $\mu\text{m}$  slit



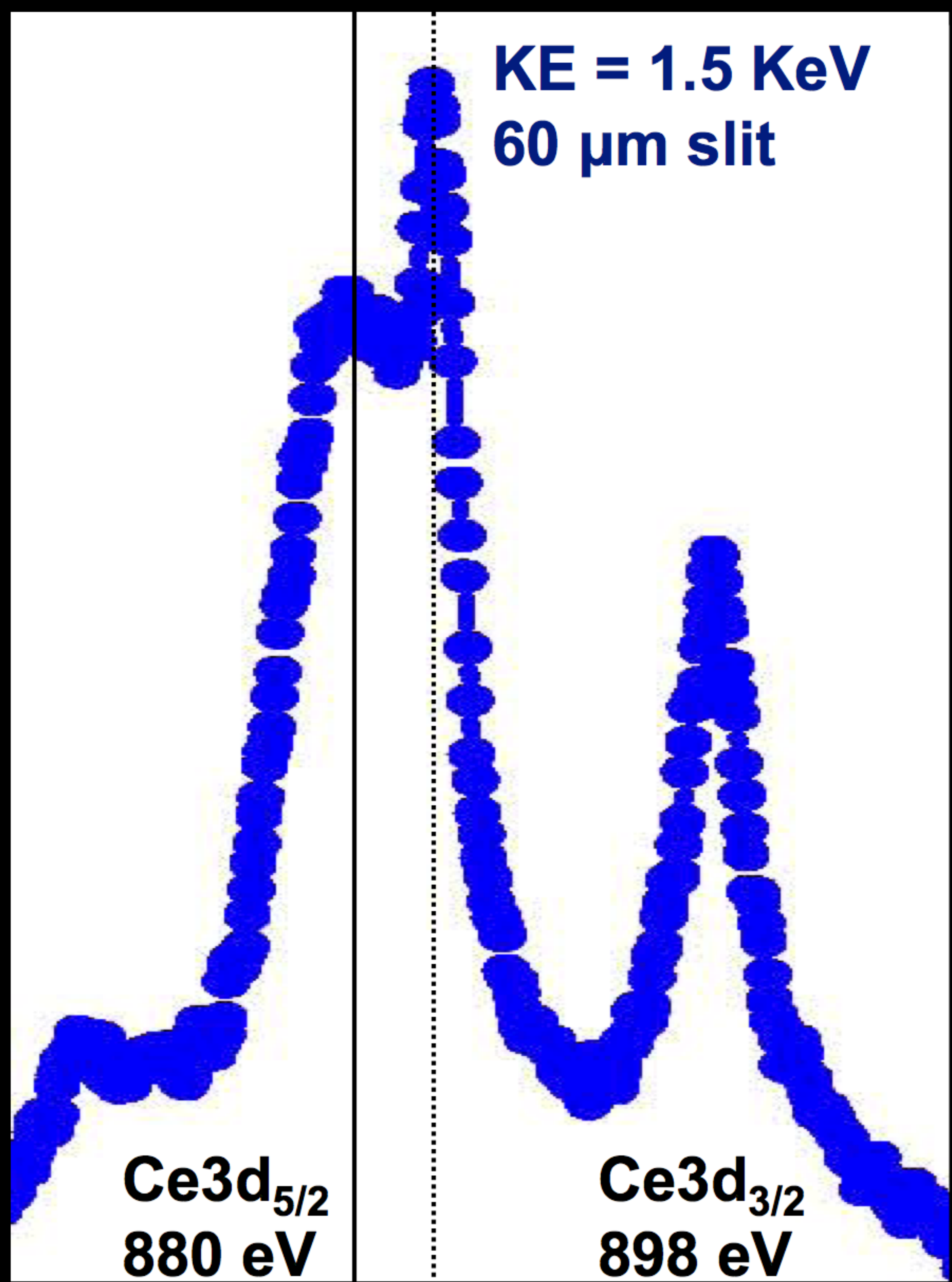
Ce  
metal

Ce  
Oxide

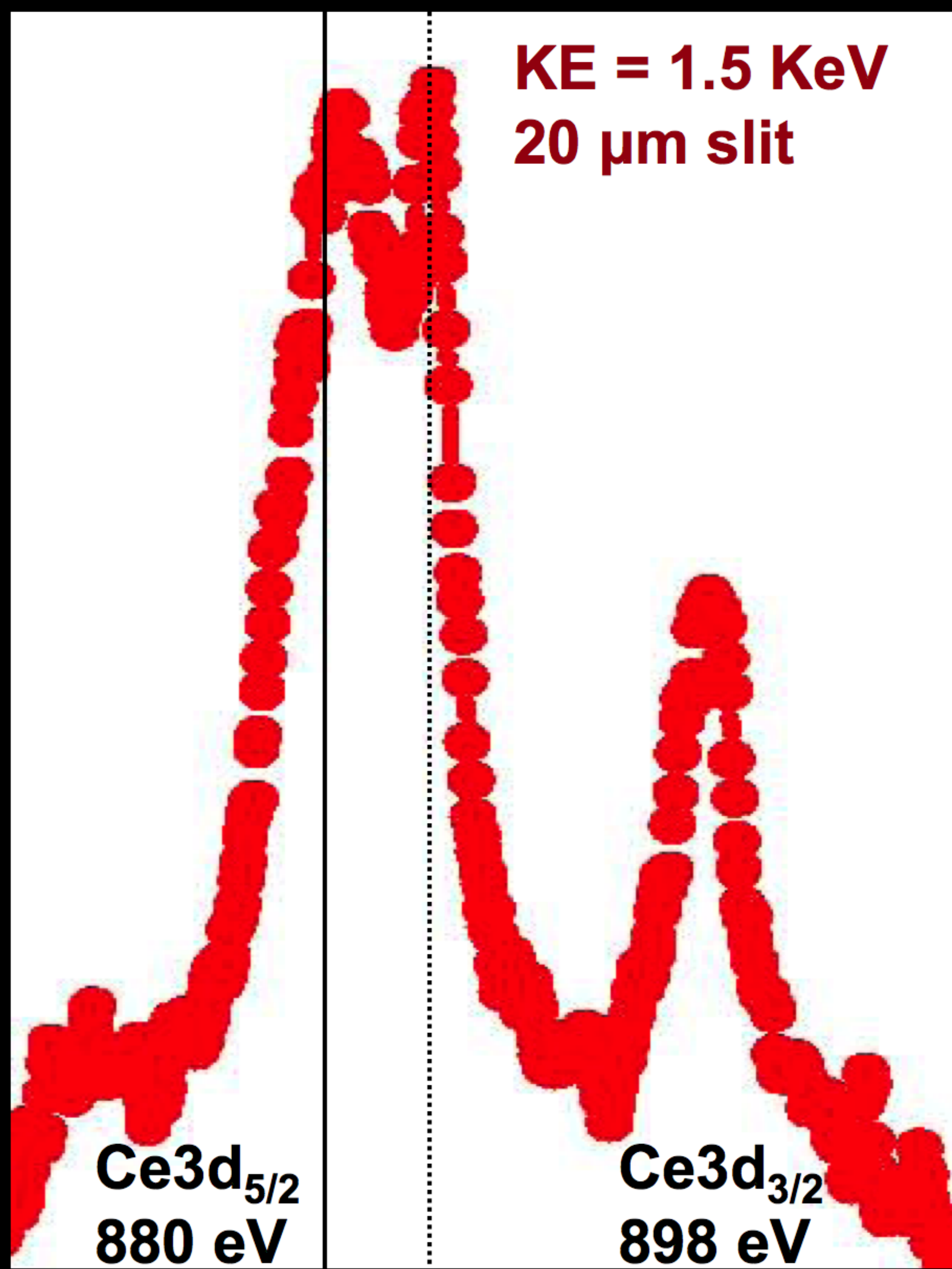
Ce  
metal

Ce  
Oxide

KE = 1.5 KeV  
60  $\mu\text{m}$  slit



KE = 1.5 KeV  
20  $\mu\text{m}$  slit



Ce3d<sub>5/2</sub>  
880 eV

Ce3d<sub>3/2</sub>  
898 eV

Ce3d<sub>5/2</sub>  
880 eV

Ce3d<sub>3/2</sub>  
898 eV

860

hv(eV)

910

860

hv(eV)

910

# CeOxide O1s XES

Intensity (Arb. Units)

- Slits 60 $\mu$ m, KE = 3.0KeV
- Slits 60 $\mu$ m, KE = 1.5KeV
- Slits 20 $\mu$ m, KE = 3.0KeV
- Slits 20 $\mu$ m, KE = 1.5KeV

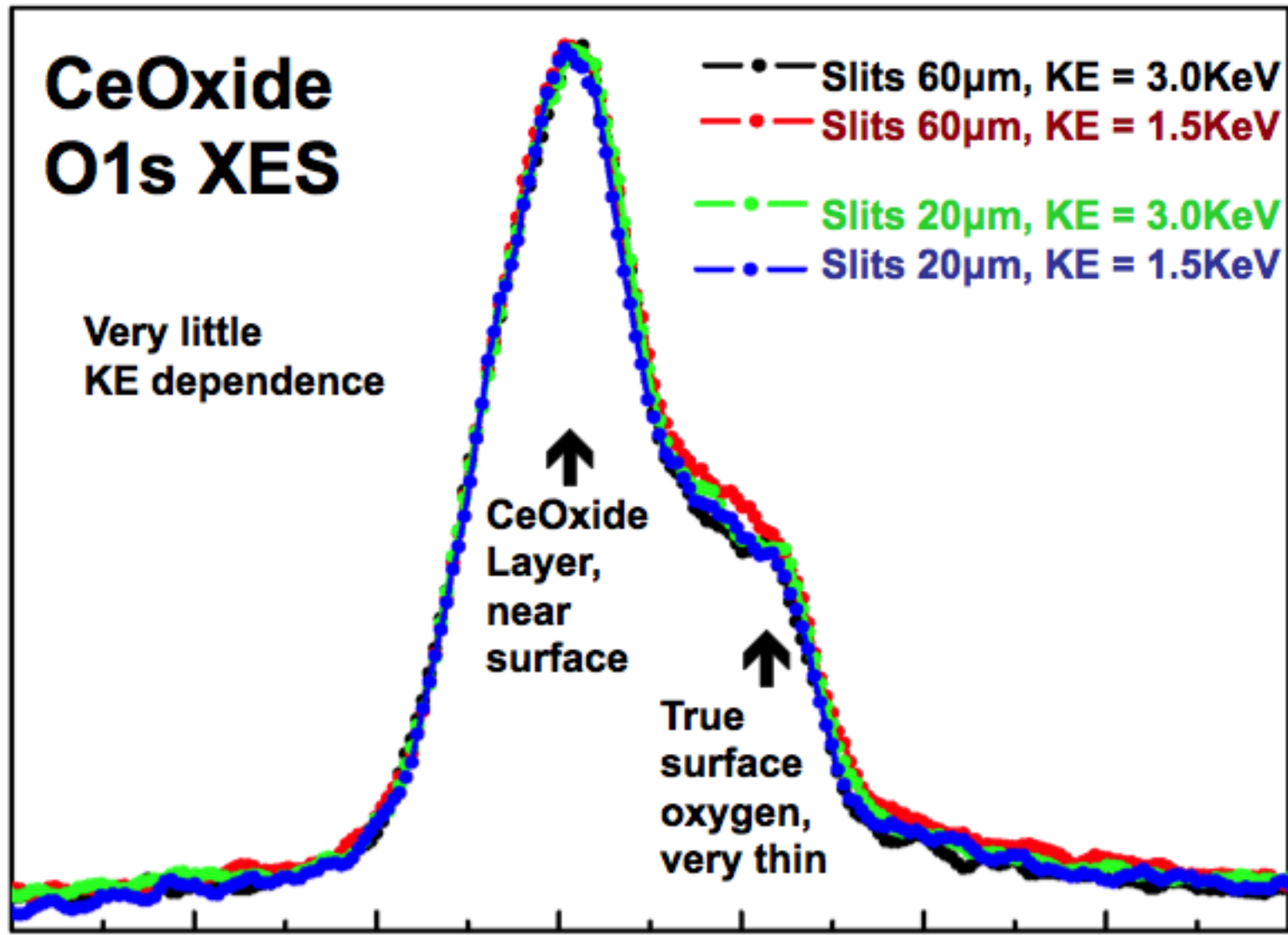
Very little  
KE dependence

↑  
CeOxide  
Layer,  
near  
surface

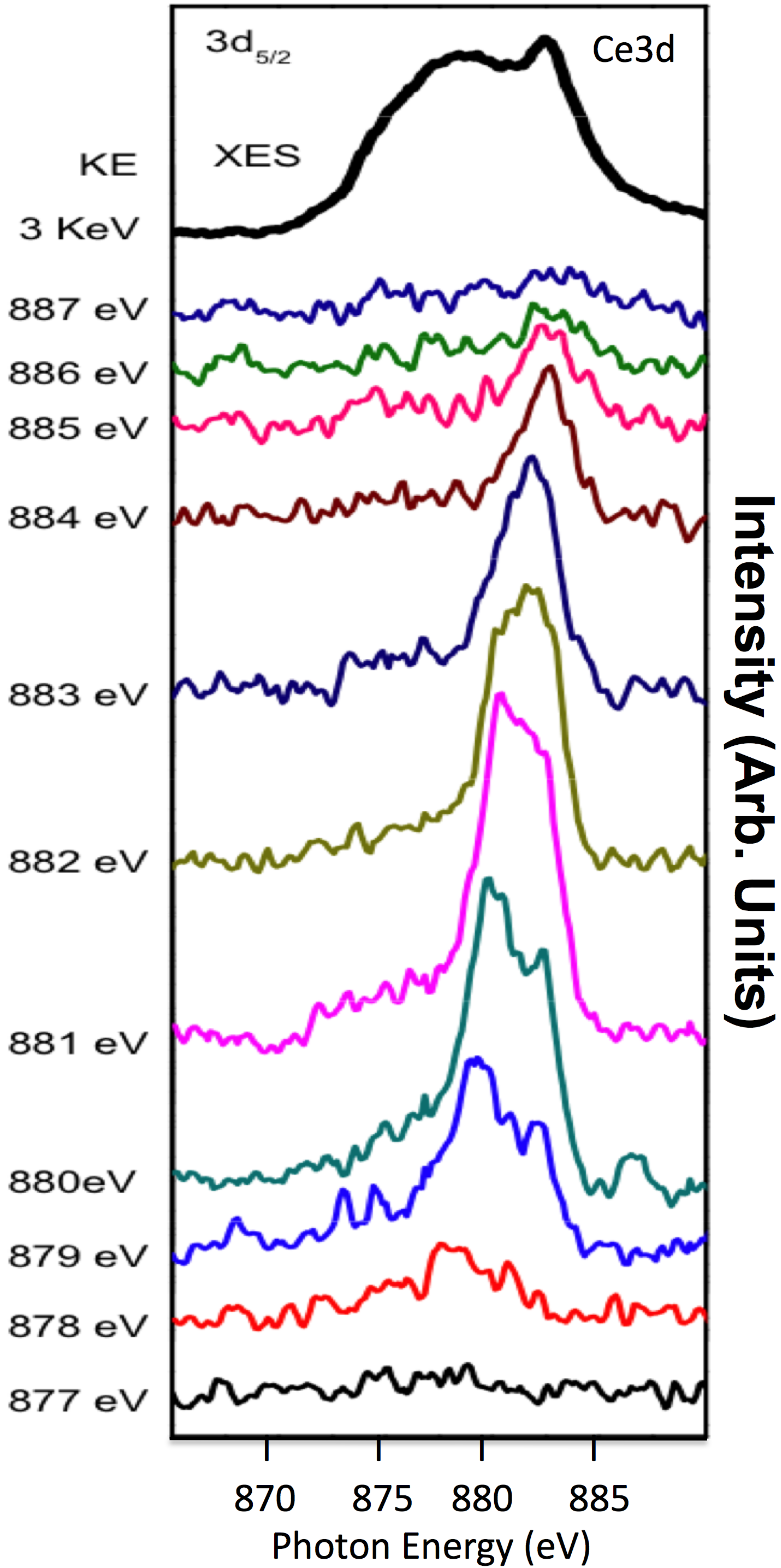
↑  
True  
surface  
oxygen,  
very thin

518 520 522 524 526 528 530 532

Photon Energy (eV)



# RIPES of CeOxide



# RIPES of CeOxide

